PHYSICAL REVIEW E **77**, 060903(R) (2008)

Activity-dependent stochastic resonance in recurrent neuronal networks

Vladislav Volman[1,2,*] and Herbert Levine[1]

[1]*Center for Theoretical Biological Physics, University of California at San Diego, La Jolla, California 92093-0319, USA*

[2]*Computational Neurobiology Laboratory, The Salk Institute for Biological Studies, La Jolla, California 92037, USA*

(Received 17 February 2008; published 20 June 2008)

We use a biophysical model of a local neuronal circuit to study the implications of synaptic plasticity for the detection of weak sensory stimuli. Networks with fast plastic coupling show behavior consistent with stochastic resonance. The addition of an additional slow coupling that accounts for the asynchronous release of neurotransmitter results in qualitatively different properties of signal detection, and also leads to the appearance of transient post-stimulus bistability. Our results suggest testable hypothesis with regard to the self-organization and dynamics of local neuronal circuits.

DOI: 10.1103/PhysRevE.77.060903 PACS number(s): 87.19.ll, 87.19.lv, 87.85.Ng, 89.75.Fb

Stochastic resonance (SR) refers to the condition in which noise and nonlinearity combine to amplify otherwise undetectable stimuli [1]. This simple, yet important, phenomenon has received much attention due to its apparent ubiquity in many nonlinear abiotic [1] and biological [2] systems. In particular, a number of studies have raised the possibility that neurons [3,4] and neuronal cell assemblies [5] might utilize SR in order to detect weak sensory stimuli [2].

For these studies, the noise felt by individual neurons has been assumed to arise from the random summation of a large number of synaptic stimuli [4,6]. There is, however, another important source of noise, that of the stochastic nature of synaptic transmission. In particular, there can occur spontaneous asynchronous release (AR) of neurotransmitter at a rate that is strongly dependent on the presynaptic Ca^{2+} concentration and hence strongly dependent on the rate of spike-induced Ca^{2+} intake [7]. Since a high probability of release can last for >0.1 s, AR constitutes a challenging example of slow time-scale, activity-dependent noise.

The purpose of this work is to show that SR for *local* circuits consisting of roughly 100 neurons (a "microcolumn" [8]) coupled via noisy plastic synapses takes a dramatically different form from that seen in investigations to date. As we will see, the coherence of the response continues to depend nontrivially on the coupling strength and the assembly size. Furthermore, the circuit can exhibit short-term memory, by which we mean that spiking will continue to occur for a transient period following removal of the stimulus. These results can be directly tested in experiments on cultured networks [7,9] and offer some insights into the way neuronal systems can be organized for optimal information processing. From the dynamical systems point of view, this work represents an example of how SR phenomenology can depend on the specific type of noise; this has been considered in only a few examples to date [10].

To proceed, we use a network model that has recently been developed to account for the occurrence of rhythmic reverberatory responses in hippocampal cultures [7,11]. The neurons in the network obey Morris-Lecar-like dynamics [12] with the membrane voltage given by

$$C\dot{V} = -I_{\text{ion}} + I_{\text{bg}} + I_{\text{syn}} + I_{\text{stim}}. \tag{1}$$

In Eq. (1), the ionic current I_{ion} describes the contribution from membrane channels [13]. The term I_{bg} is a background current that represents summation of a large number of synaptic stimuli from neurons that are not part of the specific local circuit. Rather than explicitly modeling a very large network and imposing a connectivity pattern that embodies the local circuit notion, we instead include these neurons *implicitly* by assuming (as in [6]) that their contribution is described by a Langevin equation $\dot{I}_{\text{bg}} = -I_{\text{bg}}/\tau_n + \sqrt{D/\tau_n}\mathcal{N}(0,1)$, with $\tau_n = 10$ ms and $\mathcal{N}(0,1)$ being uncorrelated Gaussian noise with zero mean and unitary variance. The synaptic current due to the local circuit is modeled as $I_i^{\text{syn}} = -\Sigma \bar{g} Y_{ij}(t) V_i$, with $\bar{g} \in [0.5, 0.8]$ mS/cm^2 being the maximal value of synaptic conductance, the sum running over the set of input channels, and the term Y_{ij} as described below. With the parameters as given in [13], the transition from quiescence to regular spiking occurs through a Hopf bifurcation.

To capture the dynamical aspects of synaptic coupling, we assume that at any time, presynaptic resources can be in a recovered state (described by the state variable X in equations below), in an active state (described by the state variable Y), or in an inactive state (described as $Z = 1 - X - Y$) [14]. The dynamics for the $j \to i$ presynaptic terminal are

$$\dot{X}_{ij} = \frac{Z_{ij}}{\tau_r} - X_{ij}[U\delta(t - t_s^j) + \xi\delta(t - t_a^j)], \tag{2a}$$

$$\dot{Y}_{ij} = \frac{-Y_{ij}}{\tau_d} + X_{ij}[U\delta(t - t_s^j) + \xi\delta(t - t_a^j)], \tag{2b}$$

$$\dot{Z}_{ij} = \frac{Y_{ij}}{\tau_d} - \frac{Z_{ij}}{\tau_r}, \tag{2c}$$

$$\eta(c) = \eta_{\max}\frac{c^4}{c^4 + K_a^4}, \tag{2d}$$

$$\dot{c} = \frac{-\beta c^2}{c^2 + K_{Ca}^2} + \gamma \log\left(\frac{c_o}{c}\right)\delta(t - t_s^j) + I_p. \tag{2e}$$

*Author to whom correspondence should be addressed: volman@salk.edu

At each presynaptic terminal of the ith neuron, the fraction of active resources (Y_{ij}) experiences a brief increase of magnitude UX_{ij} when, at time t_s^j, an action potential from the jth neuron invades the presynaptic terminal. Alternatively, a relatively small amount of resource can be maintained in an active state by the asynchronous release of synaptic resource that occurs at times t_a^j with Ca^{2+}-dependent rate $\eta(c)$ and amplitude ξ. The rate of asynchronous release (probability to observe an event during the interval $[t_a, t_a+dt]$, modeled as the Poisson process) is taken to be a Hill function of the presynaptic residual Ca^{2+} concentration, c [11,15]. This residual Ca^{2+} accumulates at presynaptic terminals in an activity-dependent way that is proportional to the electrochemical gradient across the membrane, and is extruded into the extracellular space by a nonlinear pump. The term I_p ensures that the minimal Ca^{2+} concentration is $\approx$60 nM. Parameters are given in [16]. Note that the phasic (UX_{ij}) and asynchronous (ξX_{ij}) terms are both proportional to the amount of available resource, X_{ij}, underscoring the activity-dependent competition between these two different coupling modes [17].

To assess the extent to which an individual neuron and/or a network can exhibit coherent activity, we use the coherence of spiking (COS) measure [4,18]. Given a weak external subthreshold stimulation of period T, $I_{\text{stim}}(t)=1\frac{\text{nA}}{\text{cm}^2}\sin(2\pi\frac{t}{T})$, the

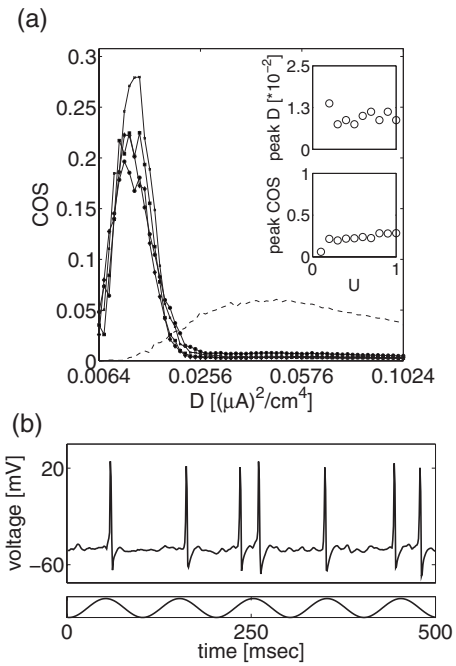

FIG. 1. Stochastic resonance in dynamically coupled neuronal networks. (a) An uncoupled cell ensemble exhibits a broad-peak stochastic resonance with relatively weak coherence of spiking (dashed line). Introduction of dynamic coupling enables the efficient exchange of stimulus-related information, and moves the resonance peak to lower noise intensities. Once above a minimal coupling threshold, different coupling strengths induce nearly the same coherence-noise curves (superimposed lines). Both optimal noise intensity (top inset) and peak coherence (bottom inset) are nearly independent of synaptic coupling. (b) Sample neuronal membrane voltage for $D=1.25\times10^{-2}$, $U=0.4$, and $\eta_{\max}=0$.

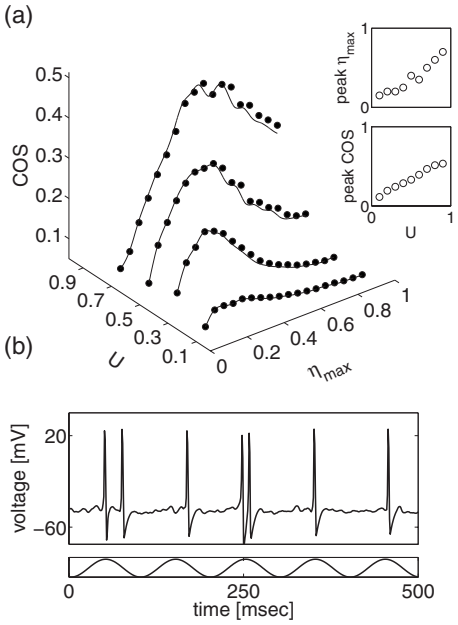

FIG. 2. Stochastic resonance in a network with asynchronous release of transmitter. (a) When a slow asynchronous mode of synaptic transmission is introduced in addition to the fast phasic coupling, the extent of output spiking coherence depends on the strength of the phasic coupling (U). For clarity of presentation, only the cases $U=0.1$, 0.3, 0.5, and 0.7 are shown. Both the location (top inset) and magnitude (bottom inset) of the coherence peak are positively correlated with the strength of evoked synaptic transmission, underscoring the fact that both kinds of synaptic transmission share the same pool of synaptic resources. (b) Sample neuronal membrane voltage for $\eta_{\max}=0.28$, $U=0.4$, and $D=0.64\times10^{-2}$.

COS measure C_S is defined here as $C_S\equiv\frac{N(0.9T<=\text{ISI}<=1.1T)}{N(\text{ISI})}$, that is, the fraction of interspike intervals (ISIs) that are within 20% of the stimulus period, $T=0.1$ s. All results, unless otherwise indicated, are for a network of $N=100$ neurons that have probability $p=0.1$ to establish connections with their peers.

We first analyze the response of an uncoupled neuronal network to weak subthreshold periodic stimulation and different (controlled) intensities of synaptic background noise, I_{bg}. In agreement with previous studies [3], we find that there exists an optimal level of noise for which a model neuron exhibits a maximal coherence of spiking [Fig. 1(a), dashed line]. Coupling the model neurons by activity-dependent synapses [as in Eqs. (2)] while setting $\eta_{\max}=0$ (no asynchronous release) moves the resonant peak toward lower noise intensities. As Fig. 1(a) (insets) shows, the location and the height of the new peak are largely independent of the coupling parameter, U. This observation is consistent with the notion of efficient signal propagation on random graphs—once U is above the critical coupling threshold, a SR-like activation of one neuron will quickly spread the word to other neurons, regardless of the exact value of U.

Introduction of activity-dependent asynchronous release of neurotransmitter results in a qualitatively different picture. The coherence measure as a function of evoked and asynchronous release is shown in Fig. 2(a). It is clear that the spiking coherence increases significantly for higher values of

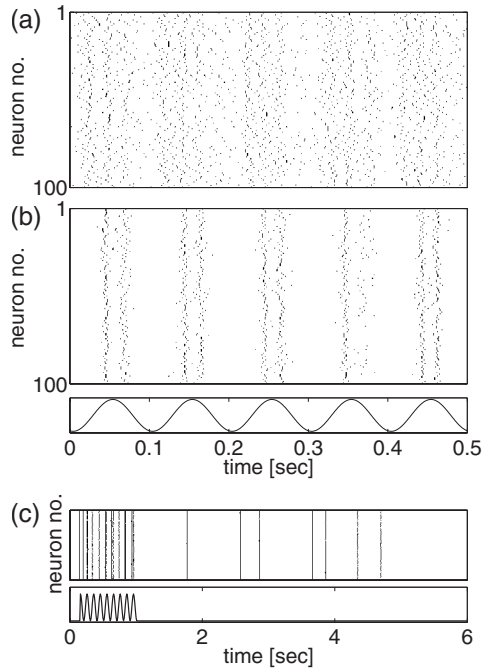

FIG. 3. AR induces correlated collective dynamics. Raster plots show the firing activity of a neuronal network with $U=0.4$. (a) A network with $D=7.84\times10^{-2}$, $\eta_{max}=0$ exhibits high-rate, uncorrelated activity. On the contrary, a network with $D=0$, $\eta_{max}=0.8$ (b) exhibits burstlike, correlated collective activity. (c) A network driven by AR shows transient bistability in its activity (top panel) that persists for seconds after stimulus removal (bottom panel).

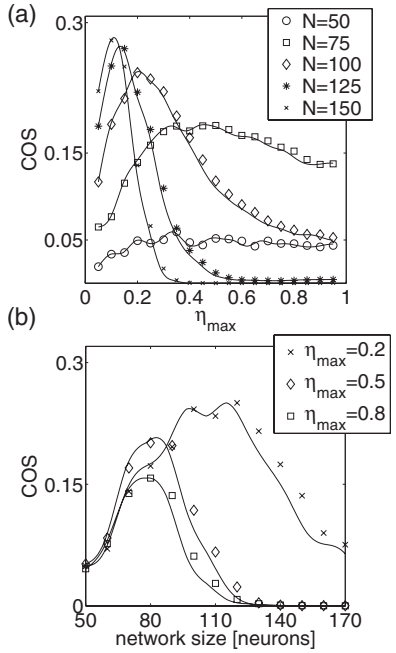

FIG. 4. System size and connectivity affect coherence of spiking. (a) For a network with a uniform connection probability ($p=0.1$), the profile of coherence as a function of maximal AR rate depends on the number of neurons. With a $p=$const scheme, larger networks lead to higher per cell number of afferents that affects the effective level of asynchronous release. (b) Optimal network size (peaks) that gives rise to maximal coherence depends on the maximal rate of AR at model synapses. In all cases, the intensity of background synaptic noise is $D=0.64\times10^{-2}$.

the resource utilization parameter U. The optimal level of AR needed to produce maximal coherence [peaks in Fig. 2(a)] also depends on the value of U. Stronger evoked transmission will quickly deplete the available resources; therefore, since asynchronous and evoked releases draw from the same pool of vesicles, a higher rate of spontaneous events is needed to achieve significant spiking coherence [top inset of Fig. 2(a)]. For higher values of η_{max}, when the combined action of AR and I_{bg} masks the stimulus by making the cell spike more frequently, the coherence measure converges to low values. On the other hand, strong coupling and fast depletion of resources provide a constraint for spiking activity, resulting in higher overall coherence for higher resource usage [bottom inset of Fig. 2(a)].

The distinctive effect of AR (as compared with I_{bg}) is further assessed by analyzing the collective dynamics for high η_{max} (vs high D). Subjecting the network to high-intensity dynamics-independent noise [Fig. 3(a)] results in high-rate, weakly correlated, activity. On the other hand, as Fig. 3(b) shows, the combined action of strong AR and synaptic depression significantly sharpens the network's response to the stimulus. Further, the prolonged time scale of AR enables the network to "remember" the stimulus seconds after its cessation [Fig. 3(c)].

The observation that coherence of spiking depends on the strength of dynamic coupling prompted us to explore how a network's parameters affect its ability to detect weak stimuli. To this end, we considered the performance of different size networks, for a range of AR rates. For easier interpretation of results, we assume here that, for all cases, $U=0.3$. Figure 4(a) shows that the profiles of COS curves are different for different network sizes. Due to the $p=$const constraint, neurons in larger networks are subject to higher levels of asynchronous release in their inputs; as a result, the resonant peak moves toward lower values of η_{max}. Conversely, fixing the value of η_{max} and plotting the COS measure as a function of network size [as is in Fig. 4(b)] reveals that the optimal network size (giving maximal coherence) depends on the level of AR at individual model synapses. Thus, in a network with plastic coupling, synaptic parameters might provide constraints for the sizes of cell assembly.

Stochastic resonance relies on the cooperativity between noise, nonlinearity, and a weak subthreshold stimulus [1]. In most examples, the noise is taken to be independent of the characteristics of the weak subthreshold stimulus (but see [10]). Here, we have investigated the properties of signal processing in local recurrent neuronal networks with plastic coupling and asynchronous release of neurotransmitter, where the noise is inherently coupled to the signal. We found that in plastic networks without AR, the characteristics of stochastic resonance (location and height of peak coherence) depend only weakly on the strength of synaptic coupling. On the contrary, introduction of AR leads to a strong dependence of SR properties on network parameters.

These observations suggest that asynchronous release of neurotransmitter might play an important role in neuronal dynamics [19]. Information that is contained in weak signals

should not only be detected and amplified by brain circuitry; a network has to have the ability to transiently "hold" knowledge about preceding events. As shown in [7,11], a brief stimulus delivered to the network evokes reverberatory activity that is sustained by the asynchronous release of neurotransmitter and lasts for several seconds. Our results [Fig. 3(c)], together with experimental observations [7] and prior modeling [11], suggest that AR can be instrumental in detection, amplification, and transient holding of weak sensory stimuli.

This study leads to several potentially interesting conclusions. First, we showed here that the ability of a neuron (that is embedded in a neuronal network) to detect and amplify weak stimuli might depend crucially on the form of feedback from the network, and in particular on the plasticity features of the effective connectivity. Second, our results suggest that the plasticity of synaptic connections might provide an important constraint for the optimal number of neurons in a local circuit. With this perspective, the local network with strong interconnectivity is optimized for signal detection, with distant neurons providing contextual information in the form of an overall background noise signal. Cultured networks can provide an adequate framework to test the validity of our conclusions. State of the art techniques allow one to grow small networks of controlled size, geometry, and connectivity [9]. Future experiments will determine how these parameters affect the ability of a network to process weak stimuli.

We thank W. J. Rappel and T. J. Sejnowski for stimulating discussions. This research has been supported by the NSF-sponsored Center for Theoretical Biological Physics (Grants No. PHY-0216576 and No. PHY-0225630).

[1] L. Gammaitoni *et al.*, Rev. Mod. Phys. **70**, 223 (1998).

[2] R. J. Douglas *et al.*, Nature **365**, 337 (1993); J. J. Collins *et al.*, J. Neurophysiol. **76**, 642 (1996); J. E. Levin and J. P. Miller, Nature **380**, 165 (1996); B. Gluckman *et al.*, Phys. Rev. Lett. **77**, 4098 (1996); F. Jaramillo and K. Wiesenfeld, Nat. Neurosci. **1**, 384 (1998); W. C. Stacey and D. M. Durand, J. Neurophysiol. **83**, 1394 (2000); F. Moss *et al.*, Clin. Neurophysiol. **115**, 267 (2004).

[3] A. Longtin, J. Stat. Phys. **70**, 309 (1993).

[4] M. Rudolph and A. Destexhe, Phys. Rev. Lett. **86**, 3662 (2001).

[5] A. R. Bulsara and G. Schmera, Phys. Rev. E **47**, 3734 (1993); W. J. Rappel and A. Karma, Phys. Rev. Lett. **77**, 3256 (1996); D. Chialvo, A. Longtin, and J. Muller-Gerking, Phys. Rev. E **55**, 1798 (1997); G. Mato, *ibid.* **58**, 876 (1998); Y. Yu, W. Wang, J. Wang, and F. Liu, *ibid.* **63**, 021907 (2001); C. Zhou, J. Kurths, and B. Hu, Phys. Rev. Lett. **87**, 098101 (2001).

[6] A. Destexhe *et al.*, Neuroscience **107**, 13 (2001).

[7] P. Lau and G. Bi, Proc. Natl. Acad. Sci. U.S.A. **102**, 10333 (2005).

[8] E. G. Jones, Proc. Natl. Acad. Sci. U.S.A. **97**, 5019 (2000).

[9] R. Sorkin *et al.*, J. Neural Eng. **3**, 95 (2007).

[10] S. Bezrukov and I. Vodyanoy, Nature **385**, 319 (1997); B. Lindner and L. Schimansky-Geier, Phys. Rev. Lett. **86**, 2934 (2001).

[11] V. Volman *et al.*, Phys. Biol. **4**, 91 (2007).

[12] C. Morris and H. Lecar, Biophys. J. **35**, 193 (1981); S. A. Prescott *et al.*, J. Neurosci. **25**, 9084 (2006).

[13] For each model neuron, the ionic current was $I_{\text{ion}}=G_{\text{Na}}m_{\infty}(V-E_{\text{Na}})+G_K w(V)(V-E_K)+G_L(V-E_L)$. The fraction of open K^+ channels evolved as $dw/dt=0.15[w_{\infty}(V)-w(V)]\cosh[(V-V_3)/2V_4]$. The steady-state fractions of Na^+ and K^+ channels were, correspondingly, $m_{\infty}=0.5\{1+\tanh[(V-V_1)/V_2]\}$ and $w_{\infty}=0.5\{1+\tanh[(V-V_3)/V_4]\}$. Values of the parameters were $E_{\text{Na}}=50$ mV, $E_K=-100$ mV, $E_L=-55.8$ mV, $V_1=-1.2$ mV, $V_2=23$ mV, $V_3=-2$ mV, $V_4=21$ mV, $G_{\text{Na}}=11$ mS/cm^2, $G_K=10$ mS/cm^2, $G_L=1.5$ mS/cm^2, and $C=1$ μF/cm^2. Equations were solved using the second-order Runge-Kutta method with $dt=0.1$ ms.

[14] M. Tsodyks *et al.*, J. Neurosci. **20**, RC50(1–5) (2000).

[15] R. Ravin *et al.*, J. Physiol. (London) **501**, 251 (1997); S. Kirischuk and R. Grantyn, *ibid.* **548**, 754 (2003).

[16] The parameters used to model synaptic transmission were $\tau_d=5$ ms, $\tau_r=0.6$ s, $K_a=0.1$ μM, $K_{\text{Ca}}=0.4$ μM, $\beta=2$ μM/s, $\gamma=80$ nM, $C_0=2$ mM, $I_p=0.11$ μM/s, and $\xi=10^{-3}$.

[17] D. Hagler and Y. Goda, J. Neurophysiol. **85**, 2324 (2001); Y. Otsu *et al.*, J. Neurosci. **24**, 420 (2004).

[18] D. R. Chialvo and A. V. Apkarian, J. Stat. Phys. **70**, 375 (1993).

[19] J. Jones *et al.*, J. Neurophysiol. **97**, 3812 (2007); K. J. Iremonger and J. S. Bains, J. Neurosci. **27**, 6684 (2007).